Sublattice modulated superconductivity in the kagome Hubbard model

Tilman Schwemmer,[1,2,*] Hendrik Hohmann,[1,2,*] Matteo Dürrnagel,[1,2,3,*] Janik Potten,[1,2] Jacob Beyer,[1,4,5,6] Stephan Rachel,[4] Yi-Ming Wu,[7] Srinivas Raghu,[7] Tobias Müller,[1,2] Werner Hanke,[1,2] and Ronny Thomale[1,2,8,†]

[1]*Institute for Theoretical Physics, Julius-Maximilians-Universität Würzburg, 97074 Würzburg, Germany*
[2]*Würzburg-Dresden Cluster of Excellence ct.qmat, University of Würzburg, 97074 Würzburg, Germany*
[3]*Institute for Theoretical Physics, ETH Zürich, 8093 Zürich, Switzerland*
[4]*School of Physics, University of Melbourne, Parkville, Victoria 3010, Australia*
[5]*Institute for Theoretical Solid State Physics, RWTH Aachen University, 52062 Aachen, Germany*
[6]*JARA Fundamentals of Future Information Technology, 52062 Aachen, Germany*
[7]*Stanford Institute for Theoretical Physics, Stanford University, Stanford, California 94305, USA*
[8]*Department of Physics and Quantum Centers in Diamond and Emerging Materials (QuCenDiEM) group, Indian Institute of Technology Madras, Chennai 600036, India*

(Received 23 March 2023; revised 8 April 2024; accepted 20 May 2024; published 1 July 2024)

We identify a superconducting order featuring spatial pair modulations on the kagome lattice subject to on-site Hubbard U and nearest-neighbor V interactions. Within our functional renormalization group analysis, this state appears with a concomitant d-wave superconducting (SC) instability at zero lattice momentum, where it distinguishes itself through *intra-unit-cell modulations* of the pairing function thus breaking the discrete space group symmetry. The relative weight of the sublattice modulated superconductor (SMS) and d-wave SC is influenced by the absolute interaction strength and coupling ratio V/U. Parametrically adjacent to this domain at weak coupling, we find an intra-unit-cell modulated vestigial charge density wave and an s-wave SC instability. Our study provides a microscopic setting and thorough description of this novel SMS arising within a translation symmetry broken background.

DOI: 10.1103/PhysRevB.110.024501

I. INTRODUCTION

Superconducting (SC) order beyond spatially uniform pairing is a longstanding area of condensed matter research [1]. The idea of a pair density wave (PDW), i.e., spatially varying electron pairing manifesting either as finite-range fluctuations or long-range order, has attained significant attention in the context of high-T_c cuprates [2]. There, intriguing phenomena such as Fermi arcs or layer decoupling find a rather intuitive explanation from the viewpoint of a PDW reference state. Most recently, PDWs have surfaced in experimental signatures for a plethora of material classes such as kagome metals, transition-metal dichalcogenides, heavy-fermion compound UTe_2, and pnictides [3–7], evoking a universality of the PDW state in correlated electron systems. As tempting and rich as the principal phenomenology might be, the microscopic evidence for a PDW state still is rather poor. Spatially modulated SC pairing has only been rigorously accessed in the Fulde-Ferrell-Larkin-Ovchinnikov (FFLO) scenario of subjecting weak-coupling spin-singlet SC to a magnetic field [8,9]. Without an external field, there is no generic weak-coupling solution featuring Cooper pairs at finite lattice momentum. Therefore, the majority of previous attempts had to resort to effective mean-field treatments either through postulating finite-range bare pair hopping [10] or analyzing higher-order terms of Ginzburg-Landau expansions [11–13]. It is then usually a matter of nonuniversal parameter choice whether one finds a PDW as competing order to uniform SC and charge density wave (CDW), or as a, possibly fluctuating, high-temperature mother state yielding vestigial SC and CDW order at lower temperature [1]. It is thus of central interest to identify a microscopic approach to correlated electron systems that realizes a PDW state [14].

The functional renormalization group (FRG) [15,16] suggests itself as a natural method to access ordering instabilities at and beyond weak coupling. Even though it lacks an analytical control parameter which is the archetypal challenge for any order at intermediate coupling, the FRG treats all bilinear fermionic orders on equal footing and allows for a smooth interpolation to the weak-coupling limit by reducing the interaction strength. FRG calculations were demonstrated to adequately describe even intricate phase diagrams of multiorbital/multisublattice correlated electron systems such as iron pnictides [17,18]. As a guiding motif for our study of spatially modulated superconductors we identify the nontrivial sublattice structure of experimentally observed PDW materials. This suggests the $U-V$ kagome Hubbard model (KHM), where U and V denote the on-site and nearest-neighbor (NN) electronic repulsion on the kagome lattice, respectively, as a blueprint to examine the sublattice structure of the low-energy fluctuations and its imprint on emergent exotic electronic orders [19,20]. In particular, the geometry of

*These authors contributed equally to this work.
†Contact author: rthomale@physik.uni-wuerzburg.de

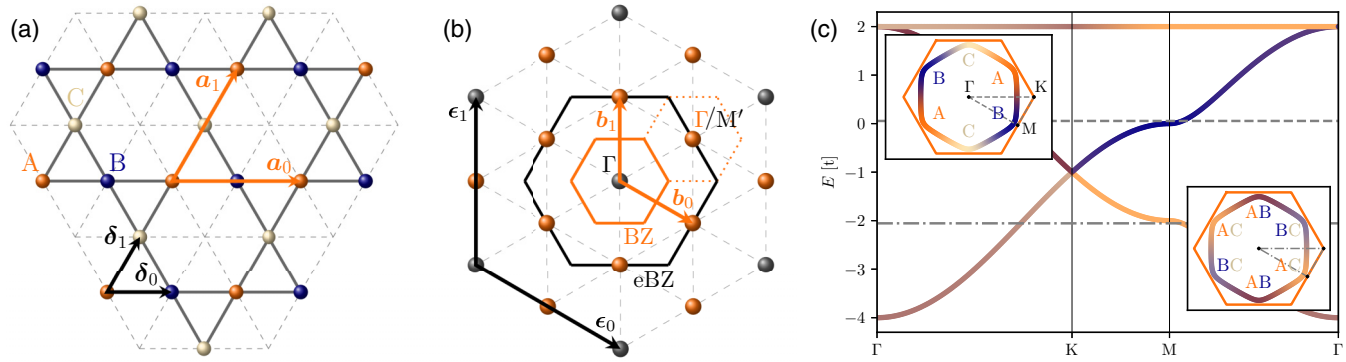

FIG. 1. Kagome fermiology and extended zone scheme. (a) Kagome lattice with sublattices A, B, and C along with the inter- ($\mathbf{a}_{0,1}$) and intra- ($\boldsymbol{\delta}_{0,1}$) unit-cell vectors. (b) Fourier transform of the kagome lattice with the Brillouin zone (BZ) in orange and extended Brillouin zone (eBZ) in black. M' points in the eBZ coincide with the Γ point in the BZ. (c) The kagome band structure features a flat band and two dispersive bands which display a particular eigenstate sublattice distribution according to sublattice interference [21]. The p-type (m-type) van Hove fillings are symbolized by dashed (dashed-dotted) lines.

the KHM promotes sublattice interference (SI) [21], leading to pronounced nonlocal interactions and emergent NN pair hopping, which creates a propensity for PDW formation [22].

Moreover, the sublattice degree of freedom allows for a formation of intra-unit-cell modulated states. In analog to an intra-unit-cell modulated charge density wave we observe a superconducting state of equal pair modulation periodicity, that hence features similar phenomenology to a PDW. However, this state does not break an additional translation symmetry but rotational symmetry within the unit cell and hence surfaces as a $\mathbf{Q} = 0$ instability in the BZ. As this deviates from the common definition of PDW, we label the obtained instability sublattice modulated superconductor (SMS).

In this paper, we develop a theory for an SMS state observed within FRG calculations. Specifically, the state we find does not appear as a parasitic onset order to another electronic instability, but unfolds as part of the leading instability in the particle-particle (pp) channel descending from a pristine kagome metallic state. In terms of symmetry classification at the pp instability level, admixes with in-plane d-wave SC (dSC) in the E_2 irreducible representation of the hexagonal point group C_{6v}. The key to disentangle the SMS from the dSC contribution is the center of mass dependence of the condensate wave function in the triatomic unit-cell basis. Here, the SMS component exhibits intra-unit-cell modulations while the dSC component is uniform.

II. KAGOME HUBBARD MODEL (KHM)

We start from

$$H = t\sum_{\langle i,j\rangle}(c^\dagger_{i\sigma}c_{j\sigma} + \text{H.c.}) + U\sum_{i=1}^{N} n_{i\uparrow}n_{i\downarrow} + \tfrac{V}{2}\sum_{\langle i,j\rangle;\sigma\sigma'} n_{i\sigma}n_{j\sigma'}, \tag{1}$$

where $c^\dagger_{i\sigma}, c_{i\sigma}$ denote electron creation and annihilation operators at site i with spin σ, $n_{i\sigma} = c^\dagger_{i\sigma}c_{i\sigma}$, and t, U, and V denote the energy scales of hopping, on-site Hubbard, and NN repulsion, respectively. The kagome lattice depicted in Fig. 1(a) features a nonbipartite lattice of corner-sharing triangles, resulting in three sublattices A, B, and C as well as Bravais lattice vectors $\mathbf{a}_0$ and $\mathbf{a}_1$. Alternatively, it can be interpreted as a charge density wave formation at 3/4 filling of an underlying triangular lattice with halved unit-cell vectors $\boldsymbol{\delta}_0$ and $\boldsymbol{\delta}_1$, where every fourth unoccupied site is projected out. In reciprocal space [Fig. 1(b)], this corresponds to the reduced (orange) and extended (black) Brillouin zone (BZ) spanned by the vectors $\mathbf{b}_{0,1}$ and $\boldsymbol{\epsilon}_{0,1}$ according to $\mathbf{b}_i^\intercal\mathbf{a}_j = \boldsymbol{\epsilon}_i^\intercal\boldsymbol{\delta}_j = 2\pi\delta_{ij}$. The three inequivalent van Hove points at the M points in the BZ epitomize a peculiar density of states of differing sublattice occupancy [pure p type at filling $n = 5/12$ for the upper and mixed m type ($n = 3/12$) for the lower van Hove level in Fig. 1(c)] [21,23], a generic feature of kagome metals which has been recently confirmed by angle-resolved photoemission spectroscopy (ARPES) [24,25]. For both m and p type, the mismatch of sublattice support for electronic eigenstates connected by van Hove point nesting triggers SI.

III. FRG INSTABILITY ANALYSIS

The FRG formulates an ultraviolet to infrared cutoff flow of the two-particle electronic vertex operator $V(\mathbf{k}_1,\mathbf{k}_2,\mathbf{k}_3,\mathbf{k}_4)c^\dagger_{\mathbf{k}_4}c^\dagger_{\mathbf{k}_3}c_{\mathbf{k}_2}c_{\mathbf{k}_1}$ as a set of differential equations, where the $\mathbf{k}_i$ denote lattice momenta. We employ the FRG in its truncated-unity (TU) approximation (TUFRG), where the vertex is separated into three different contributions according to their distinctive transfer momenta [26], which can be classified as two particle-hole (ph) and a single particle-particle (pp) channel. The complementary vertex momenta are expanded in plane-wave form factors $\phi_f(\mathbf{k}) = e^{i\mathbf{r}_f\mathbf{k}}$ via the Bravais lattice sites $\mathbf{r}_f = n\mathbf{a}_0 + m\mathbf{a}_1$, $n, m \in \mathbb{Z}$. For the KHM, any channel vertex function is specified by a 4-tuple of sublattice indices $\{o_i\}$, $i = 1,2,3,4$, transfer momentum $\mathbf{Q}$, and two residual momenta which we expand into form factors according to

$$\mathcal{V}^{\{o_i\}}_{ff'}(\mathbf{Q}) = \int_{\text{BZ}} d\mathbf{k}d\mathbf{k}' V^{\{o_i\}}(\mathbf{Q},\mathbf{k},\mathbf{k}')\phi_f(\mathbf{k})\bar{\phi}_{f'}(\mathbf{k}'). \tag{2}$$

Truncating the set of basis functions, and reflecting the locality of pp and ph pairs, this unitary expansion becomes approximate. We terminate the flow at an energy scale Λ_c, upon encountering a divergence in a vertex element indicating

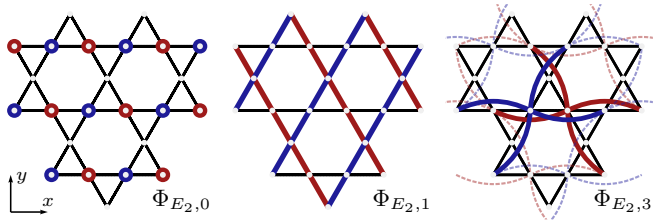

FIG. 2. Harmonics of the E_2 irrep with y-mirror eigenvalue -1. We show the on-site ($\Phi_{E_2,0}$), first NN ($\Phi_{E_2,1}$), and third NN harmonic ($\Phi_{E_2,3}$). We skip the second NN due to its similarity to the first NN. Red/blue indicates a positive/negative value of the pair correlation Eq. (4) between connected sites.

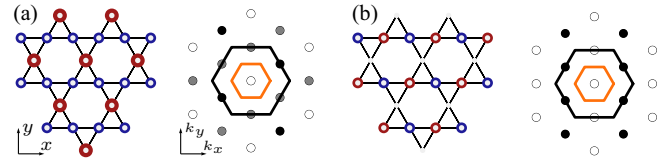

FIG. 3. Real-space representation of the two on-site pairing wave functions with E_2 symmetry and their Cooper pair momentum structure in the eBZ. Lighter shading corresponds to less intensity. Contrarily to the dSC pairing wave functions of Eq. (6), a finite Cooper pair momentum is revealed by the unfolding into the eBZ [26]. The depicted $\mathbf{Q}$ structure resembles the expected STM signature of the SMS state.

a symmetry breaking phase transition. At this point, the effective vertex contains all higher-energy quantum fluctuations accessible within the FRG approach. For SC pairing at $\mathbf{Q} = 0$, the system's ground state is then obtained from the BCS gap equation which reduces to an eigenvalue problem

$$\lambda \Delta^f_{o_1 o_2} = \sum_{f' o_3 o_4} \mathcal{V}^{\{o_i\}}_{f f'}(0) \Delta^{f'}_{o_3 o_4} \tag{3}$$

at the onset of ordering. The functional form of the SC order parameter is thus given by the eigenstate $\Delta^f_{o_1 o_2}$ associated with the most negative eigenvalue λ. Exploiting the group symmetry constraints on Eq. (3) along Schur's lemma allows for a classification of $\Delta^f_{o_1 o_2}$ in terms of irreducible representations (irreps) of C_{6v}. Within our TUFRG analysis, we identify an extended region in the $U - V$ parameter space where $\mathbf{Q} = 0$ instabilities in the spin-singlet pp channel dominate, and the superconducting order parameter transforms according to the E_2 irrep.

IV. CLASSIFICATION OF THE E_2 pp INSTABILITY

A two-electron expectation value in the spin-singlet sector,

$$\langle c^\dagger_{\mathbf{r}_i,\uparrow} c^\dagger_{\mathbf{r}_j,\downarrow} - c^\dagger_{\mathbf{r}_j,\uparrow} c^\dagger_{\mathbf{r}_i,\downarrow} \rangle = \delta_{\mathbf{r}_i,\boldsymbol{\rho}} \, \delta_{\mathbf{r}_j,\boldsymbol{\rho}} \, \Phi(\mathbf{r}_i, \mathbf{r}_j), \tag{4}$$

is most conveniently described in terms of a center-of-mass coordinate (CMC) $\mathbf{R} = (\mathbf{r}_i + \mathbf{r}_j)/2$ and a relative coordinate (RC) $\mathbf{r} = \mathbf{r}_i - \mathbf{r}_j$. In the following, we denote the set of all lattice points by $\boldsymbol{\rho}$ and use $\boldsymbol{\rho}_o$ for points related to sublattice $o \in \{A, B, C\}$. We introduce $\mathbf{a}_2 = \mathbf{a}_1 - \mathbf{a}_0$ and $\boldsymbol{\delta}_2 = \boldsymbol{\delta}_1 - \boldsymbol{\delta}_0$ for notational convenience. Since the kagome lattice is not of Bravais type, the directions of NN bonds depend on the sublattice. For each pairing distance, i.e., each value of the RC (on site, NN, etc.), the E_2 irrep is expanded in pairs of degenerate orthogonal states, characterized by even or odd transformation behavior under mirror symmetry along the y axis [26]. We order different E_2 candidate states by their RC length and constrain ourselves to the mirror-odd state as we present a graphical representation in Fig. 2. The on-site ($\mathbf{r} = 0$) pairing wave function reads

$$\Phi_{E_2,0}(\mathbf{R}, \mathbf{r}) = (\delta_{\mathbf{R},\boldsymbol{\rho}_A} - \delta_{\mathbf{R},\boldsymbol{\rho}_B}) \delta_{\mathbf{r},\mathbf{0}}. \tag{5}$$

The absence of a lattice site at the point group's rotation center allows for such on-site pairing wave functions on any non-Bravais lattice. The trivial transformation property of the RC is complemented by a nontrivial CMC function due to the reduced site symmetry group of the $3c$ Wyckoff position. In contrast, the NN pairing state

$$\Phi_{E_2,1}(\mathbf{R}, \mathbf{r}) = \delta_{\mathbf{r},\pm\boldsymbol{\delta}_1} - \delta_{\mathbf{r},\pm\boldsymbol{\delta}_2} \tag{6}$$

features a trivial CMC dependence, and instead it is the RC that captures the E_2 transformation behavior. Whereas the second NN state is structurally equivalent [26] to the NN state, the third NN pairing reads

$$\begin{aligned}\Phi_{E_2,3}(\mathbf{R}, \mathbf{r}) = {} & \delta_{\mathbf{R},\boldsymbol{\rho}_B} \delta_{\mathbf{r},\pm\mathbf{a}_0} - \delta_{\mathbf{R},\boldsymbol{\rho}_A} \delta_{\mathbf{r},\pm\mathbf{a}_0} \\ & + \delta_{\mathbf{R},\boldsymbol{\rho}_C} (\delta_{\mathbf{r},\pm\mathbf{a}_1} - \delta_{\mathbf{r},\pm\mathbf{a}_2}).\end{aligned} \tag{7}$$

It cannot be decomposed into a product of solely CMC- and RC-dependent functions. This stems from two symmetry-inequivalent types of third NN on the kagome lattice due to the reduced C_{2v} site symmetry group, that yields the additional spatial CMC structure [26].

V. SMS WAVE FUNCTION

Two candidate states may belong to the same irrep and yet trace back to entirely different physical origins. For the A_1 pairing irrep on the square lattice, this has been extensively discussed in the context of $s_\pm$- vs s_{++}-wave SC in iron pnictides [27,28]. For the kagome lattice, the fundamentally different nature of the E_2 form factors becomes apparent upon disentangling the spatial information encoded in CMC and RC, respectively. The Cooper pair wave function of typical zero momentum SCs features a uniform CMC dependence, while the RC encodes the transformation behavior of the associated irrep. Eq. (5), however, describes a scenario where the typical roles of CMC and RC are interchanged. It obeys $\sum_{\mathbf{R}} \Phi(\mathbf{R}, \mathbf{r}) = 0$, which is a characteristic of PDW-type pairing [29]. The key point to appreciate here is that despite the $\mathbf{Q} = 0$ channel, *spatially modulated contributions can be distinguished from homogeneous ones within the multisite unit cell*. This is the essential difference between the SMS and dSC contributions to an E_2 pp instability in the KHM.

Restoring the full real-space information previously encoded in the sublattice indices of the triatomic basis by transfering the SMS state of Eq. (5) to the extended BZ shown in Fig. 3 reveals finite momentum Cooper pairing, that can be directly attributed to a generalized version of the structure factor experimentally accessible in scanning tunneling microscopy (STM) measurements [for details, cf. Supplemental Material (SM) [26]]: By locally probing the differential

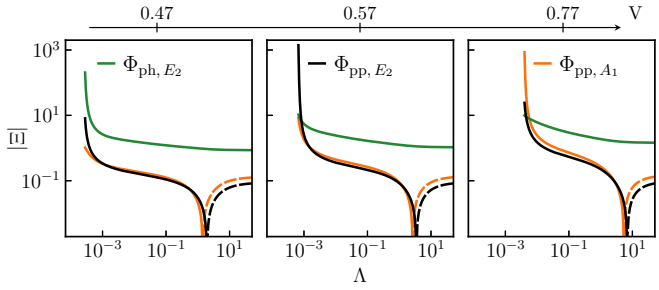

FIG. 4. FRG vertex analysis for $U/t = 0.14$ and $0.47 < V/t < 0.77$ as a function of the energy cutoff Λ. E_2 CDW (Φ_{ph,E_2}, green), SMS E_2 pp order (Φ_{pp,E_2}, black), and SC A_1 pp (Φ_{pp,A_1}, orange) compete for the leading instability. Attractive (repulsive) expectation values $|\Xi|$ of the leading instabilities at Λ_c are indicated by solid (dashed) lines [26].

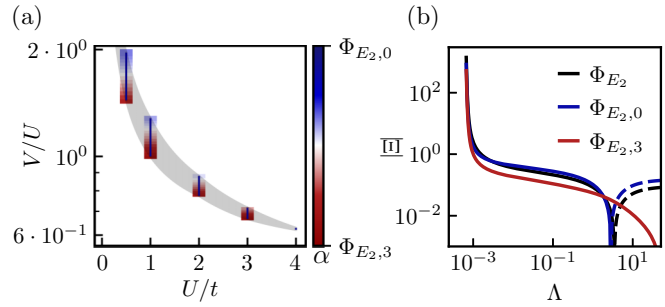

FIG. 5. (a) Admixture ratio α of $\Phi_{E_2,0}$ (blue) (5) and $\Phi_{E_2,3}$ (red) (7) for the E_2 pp domain at p-type van Hove filling ($n = 5/12$). (b) Expectation value of the leading eigenstate at Λ_c (black), $\Phi_{E_2,0}$, and $\Phi_{E_2,3}$. Negative (positive) values are indicated by solid (dashed) lines.

conductance via the Josephson tunneling signal of a superconducting STM tip, the SC gap can be monitored with high spatial resolution. The Fourier transform of the pairing gap maps exhibits peaks at the wave vectors associated with the Cooper pair modulation, that can be matched with the peak structure in Fig. 3. This allows for a clear experimental distinction between the proposed SMS state and uniform SC pairing [30–34].

VI. SMS PHASE DOMAIN

Within our TUFRG analysis of the KHM, the E_2 pp instability domain is governed by intrasublattice pairing, i.e., the eigenstates of Eq. (3) are described by a linear combination of $\Phi_{E_2,0}$ and $\Phi_{E_2,3}$ [26]. This allows to identify the E_2 pp instability as a SMS. Such states were previously found, yet not adequately appreciated in the kagome phase diagram of Refs. [20,35]. The intrasublattice pairing tendency can be understood from the viewpoint of SI: Under the RG, effects of U are suppressed while V grows [22], making intersublattice pairing less favourable. This trend also manifests in the fact that the SMS instability at small U/t is parametrically framed by an E_2-type CDW and an A_1-type, i.e., s-wave SC (Fig. 4) at p-type van Hove filling.

The SMS state emerges as interstitial order via competing interaction processes projected into the pairing channel: U drives nonlocal spin fluctuations; V, by contrast, generates charge fluctuations entering the Cooper channel as on-site attractive interactions [36]. In Fig. 4, we illustrate the generic scenario of competing instabilities generated by this interplay of local and nonlocal interactions by comparing FRG flows for varying bare values $0.47 < V < 0.77$ at fixed $U = 0.14$, i.e., located in the weak-coupling domain. Both SMS-type and s-wave SC channels are initially repulsive (dashed lines) and subsequently turn attractive (solid lines) through the RG flow. Remarkably, the adjacent CDW features the same irrep and intrasublattice modulation as the SMS phase, suggesting vestigial symmetry-type restoration at the phase transition. In previous contexts, PDW fluctuations were similarly found to predominantly occur around phase transitions between a density wave phase and SC pairing, where a variety of competing and/or cooperative orders arise at intermediate-coupling strength [1]. Any weak-coupling theory of PDW has hitherto relied on fine-tuned fermiology [37]. Here, however, we find that the SMS prevails beyond p-type van Hove filling whenever intra-unit-cell modulations become competitive to homogeneous pairing functions due to SI.

The competition of interaction processes is directly reflected in the pairing wave functions overlap with $\Phi_{E_2,0}$ and $\Phi_{E_2,3}$ [26] and their relative weight α, which is depicted in Fig. 5(a) for the SMS regime at p-type van Hove filling. Doping slightly away from this point significantly increases the SMS region, e.g., by a factor of $\approx$2.5 for $U = 3$ at $n = 1.01 \times 5/12$. The third NN state $\Phi_{E_2,3}$ does not suffer an energy penalty from U in (1) and thus promotes attractive pairing channel already at bare coupling [Fig. 5(b)]. Analogous to the previous discussion, V-driven intra-unit-cell charge fluctuations yield an on-site attraction of Cooper pairs through the RG flow [20]. The on-site contribution $\Phi_{E_2,0}$ to SMS increases with V, and eventually drives the system into an s-wave SC.

VII. CONCLUSION AND OUTLOOK

Our findings emphasize the fundamental role of the sublattice texture on the Fermi surface in a microscopic theory of spatially modulated pairing, a motif also shared among the different PDW candidates [37–39]. The new type of sublattice modulated SC instability we find for the KHM model is facilitated by the nontrivial basis in the unit cell. This allows spatial modulations of the Cooper pair wave function, while still exploiting the Cooper logarithm of a $\mathbf{Q} = 0$ pairing instability as the main driver for the symmetry breaking transition. This establishes the proposed type of SMS as a generic instability of a Fermi liquid with sublattice degrees of freedom and may explain the broad range of materials exhibiting PDW phenomenology. The breaking of rotational symmetry instead of translational symmetry by intra-unit-cell modulations of the SC order parameter finds a direct correspondence for magnetically ordered systems in the new field of altermagnetism [40,41]. Viewing the kagome lattice as a fictitious 3/4 filling CDW of an underlying triangular lattice [Fig. 1(a)], we recover the expected intertwined character of PDW: The kagome-CDW at $2\boldsymbol{\delta}_{1,0}$ comes along with a $2\boldsymbol{\delta}_{1,0}$ PDW competing with dSC. This motif carries over to SC

within the 2×2 charge order in 135 kagome compounds [3,38]: Spatially modulated intra-unit-cell SC can arise within the enlarged 2×2 unit cell in the charge ordered phase without an additional translation symmetry breaking imposed by the SC transition. Within the SMS phase, experimental signatures of a PDW-like reciprocal Josephson effect can still be observed [42–44]. To target experimentally observed PDW states in kagome compounds such as the roton density wave reported for CsV_3Sb_5 within the charge order domain [3], the methodological shortcoming to surmount in the future is to continue the FRG flow throughout the preceding charge ordered phases [45].

ACKNOWLEDGMENTS

We thank S. A. Kivelson, M. Klett, J. B. Hauck, and M. Sigrist for discussions. The work is funded by the Deutsche Forschungsgemeinschaft (DFG, German Research Foundation) through Project-ID 258499086 - SFB 1170 and and through the Würzburg-Dresden Cluster of Excellence on Complexity and Topology in Quantum Matter–*ct.qmat* Project-ID 390858490 - EXC 2147. We acknowledge HPC resources provided by the Erlangen National High Performance Computing Center (NHR@FAU) of the Friedrich-Alexander-Universität Erlangen-Nürnberg (FAU). NHR funding is provided by federal and Bavarian state authorities. NHR@FAU hardware is partially funded by the DFG 440719683. M.D. received funding from the European Research Council under Grant No. 771503 (TopMech-Mat). S.R. was supported in part by the U.S. Department of Energy, Office of Basic Energy Sciences, Division of Materials Sciences and Engineering, under Contract No. DE-AC02-76SF00515. J.B. thanks the DFG for support through RTG 1995, within the Priority Program SPP 2244 "2DMP".

[1] D. F. Agterberg, J. S. Davis, S. D. Edkins, E. Fradkin, D. J. Van Harlingen, S. A. Kivelson, P. A. Lee, L. Radzihovsky, J. M. Tranquada, and Y. Wang, The physics of pair-density waves: Cuprate superconductors and beyond, Annu. Rev. Condens. Matter Phys. **11**, 231 (2020).

[2] E. Fradkin, S. A. Kivelson, and J. M. Tranquada, *Colloquium:* Theory of intertwined orders in high temperature superconductors, Rev. Mod. Phys. **87**, 457 (2015).

[3] H. Chen, H. Yang, B. Hu, Z. Zhao, J. Yuan, Y. Xing, G. Qian, Z. Huang, G. Li, Y. Ye, S. Ma, S. Ni, H. Zhang, Q. Yin, C. Gong, Z. Tu, H. Lei, H. Tan, S. Zhou, C. Shen *et al.*, Roton pair density wave in a strong-coupling kagome superconductor, Nature (London) **599**, 222 (2021).

[4] X. Liu, Y. X. Chong, R. Sharma, and J. C. S. Davis, Discovery of a Cooper-pair density wave state in a transition-metal dichalcogenide, Science **372**, 1447 (2021),.

[5] Q. Gu, J. P. Carroll, S. Wang, S. Ran, C. Broyles, H. Siddiquee, N. P. Butch, S. R. Saha, J. Paglione, J. C. S. Davis, and X. Liu, Detection of a pair density wave state in UTe_2, Nature (London) **618**, 921 (2023).

[6] H. Zhao, R. Blackwell, M. Thinel, T. Handa, S. Ishida, X. Zhu, A. Iyo, H. Eisaki, A. N. Pasupathy, and K. Fujita, Smectic pair-density-wave order in $EuRbFe_4As_4$, Nature (London) **618**, 940 (2023).

[7] H. Li, D. Oh, M. Kang, H. Zhao, B. R. Ortiz, Y. Oey, S. Fang, Z. Ren, C. Jozwiak, A. Bostwick, E. Rotenberg, J. G. Checkelsky, Z. Wang, S. D. Wilson, R. Comin, and I. Zeljkovic, Small Fermi pockets intertwined with charge stripes and pair density wave order in a kagome superconductor, Phys. Rev. X **13**, 031030 (2023).

[8] P. Fulde and R. A. Ferrell, Superconductivity in a strong spin-exchange field, Phys. Rev. **135**, A550 (1964).

[9] A. I. Larkin and Y. N. Ovchinnikov, Nonuniform state of superconductors, Zh. Eksp. Teor. Fiz. **47**, 1136 (1964) [Sov. Phys. JETP **20**, 762 (1965)].

[10] F. Loder, A. P. Kampf, and T. Kopp, Superconducting state with a finite-momentum pairing mechanism in zero external magnetic field, Phys. Rev. B **81**, 020511(R) (2010).

[11] E. Berg, E. Fradkin, and S. A. Kivelson, Charge-4*e* superconductivity from pair-density-wave order in certain high-temperature superconductors, Nat. Phys. **5**, 830 (2009).

[12] D. F. Agterberg and H. Tsunetsugu, Dislocations and vortices in pair-density-wave superconductors, Nat. Phys. **4**, 639 (2008).

[13] P. A. Lee, Amperean pairing and the pseudogap phase of cuprate superconductors, Phys. Rev. X **4**, 031017 (2014).

[14] Y.-M. Wu, P. A. Nosov, A. A. Patel, and S. Raghu, Pair density wave order from electron repulsion, Phys. Rev. Lett. **130**, 026001 (2023).

[15] W. Metzner, M. Salmhofer, C. Honerkamp, V. Meden, and K. Schönhammer, Functional renormalization group approach to correlated fermion systems, Rev. Mod. Phys. **84**, 299 (2012).

[16] J. Beyer, J. B. Hauck, and L. Klebl, Reference results for the momentum space functional renormalization group, Eur. Phys. J. B **95**, 65 (2022).

[17] F. Wang, H. Zhai, Y. Ran, A. Vishwanath, and D.-H. Lee, Functional renormalization-group study of the pairing symmetry and pairing mechanism of the FeAs-based high-temperature superconductor, Phys. Rev. Lett. **102**, 047005 (2009).

[18] C. Platt, W. Hanke, and R. Thomale, Functional renormalization group for multi-orbital Fermi surface instabilities, Adv. Phys. **62**, 453 (2013).

[19] M. L. Kiesel, C. Platt, and R. Thomale, Unconventional Fermi surface instabilities in the kagome Hubbard model, Phys. Rev. Lett. **110**, 126405 (2013).

[20] W.-S. Wang, Z.-Z. Li, Y.-Y. Xiang, and Q.-H. Wang, Competing electronic orders on kagome lattices at van Hove filling, Phys. Rev. B **87**, 115135 (2013).

[21] M. L. Kiesel and R. Thomale, Sublattice interference in the kagome Hubbard model, Phys. Rev. B **86**, 121105(R) (2012).

[22] Y.-M. Wu, R. Thomale, and S. Raghu, Sublattice interference promotes pair density wave order in kagome metals, Phys. Rev. B **108**, L081117 (2023).

[23] X. Wu, T. Schwemmer, T. Müller, A. Consiglio, G. Sangiovanni, D. Di Sante, Y. Iqbal, W. Hanke, A. P. Schnyder, M. M. Denner, M. H. Fischer, T. Neupert, and R. Thomale, Nature of unconventional pairing in the kagome superconductors AV_3Sb_5 (A = K, Rb, Cs), Phys. Rev. Lett. **127**, 177001 (2021).

[24] M. Kang, S. Fang, J.-K. Kim, B. R. Ortiz, S. H. Ryu, J. Kim, J. Yoo, G. Sangiovanni, D. Di Sante, B.-G. Park, C. Jozwiak, A. Bostwick, E. Rotenberg, E. Kaxiras, S. D. Wilson, J.-H. Park, and R. Comin, Twofold van Hove singularity and origin of charge order in topological kagome superconductor CsV_3Sb_5, Nat. Phys. **18**, 301 (2022).

[25] Y. Hu, X. Wu, B. R. Ortiz, S. Ju, X. Han, J. Ma, N. C. Plumb, M. Radovic, R. Thomale, S. D. Wilson, A. P. Schnyder, and M. Shi, Rich nature of Van Hove singularities in Kagome superconductor CsV_3Sb_5, Nat. Commun. **13**, 2220 (2022).

[26] See Supplemental Material at http://link.aps.org/supplemental/10.1103/PhysRevB.110.024501 for details on TUFRG and further E_2 basis states, which includes Refs. [15,16,18,46–51].

[27] P. J. Hirschfeld, M. M. Korshunov, and I. I. Mazin, Gap symmetry and structure of Fe-based superconductors, Rep. Prog. Phys. **74**, 124508 (2011).

[28] A. Chubukov, Pairing mechanism in Fe-based superconductors, Annu. Rev. Condens. Matter Phys. **3**, 57 (2012).

[29] D. P. Arovas, E. Berg, S. A. Kivelson, and S. Raghu, The Hubbard model, Annu. Rev. Condens. Matter Phys. **13**, 239 (2022).

[30] J. Šmakov, I. Martin, and A. V. Balatsky, Josephson scanning tunneling microscopy, Phys. Rev. B **64**, 212506 (2001).

[31] S. H. Pan, E. Hudson, and J. Davis, Vacuum tunneling of superconducting quasiparticles from atomically sharp scanning tunneling microscope tips, Appl. Phys. Lett. **73**, 2992 (1998).

[32] T. Proslier, A. Kohen, Y. Noat, T. Cren, D. Roditchev, and W. Sacks, Probing the superconducting condensate on a nanometer scale, Europhys. Lett. **73**, 962 (2006).

[33] H. Kimura, R. P. Barber, S. Ono, Y. Ando, and R. C. Dynes, Josephson scanning tunneling microscopy: A local and direct probe of the superconducting order parameter, Phys. Rev. B **80**, 144506 (2009).

[34] S. Karan, H. Huang, C. Padurariu, B. Kubala, A. Theiler, A. M. Black-Schaffer, G. Morrás, A. L. Yeyati, J. C. Cuevas, J. Ankerhold, K. Kern, and C. R. Ast, Superconducting quantum interference at the atomic scale, Nat. Phys. **18**, 893 (2022).

[35] C. Wen, X. Zhu, Z. Xiao, N. Hao, R. Mondaini, H. Guo, and S. Feng, Superconducting pairing symmetry in the kagome-lattice Hubbard model, Phys. Rev. B **105**, 075118 (2022).

[36] A. T. Romer, S. Bhattacharyya, R. Valentí, M. H. Christensen, and B. M. Andersen, Superconductivity from repulsive interactions on the kagome lattice, Phys. Rev. B **106**, 174514 (2022).

[37] D. Shaffer, F. J. Burnell, and R. M. Fernandes, Weak-coupling theory of pair density wave instabilities in transition metal dichalcogenides, Phys. Rev. B **107**, 224516 (2023).

[38] S. Zhou and Z. Wang, Fermi pocket, topological pair density wave, and charge-4e and charge-6e superconductivity in kagomé superconductors, Nat. Commun. **13**, 7288 (2022).

[39] H.-C. Jiang, Pair density wave in the doped three-band Hubbard model on two-leg square cylinders, Phys. Rev. B **107**, 214504 (2023).

[40] I. Mazin (The PRX Editors), Editorial: Altermagnetism—a new punch line of fundamental magnetism, Phys. Rev. X **12**, 040002 (2022).

[41] L. Šmejkal, J. Sinova, and T. Jungwirth, Emerging research landscape of altermagnetism, Phys. Rev. X **12**, 040501 (2022).

[42] A. Daido, Y. Ikeda, and Y. Yanase, Intrinsic superconducting diode effect, Phys. Rev. Lett. **128**, 037001 (2022).

[43] J. J. He, Y. Tanaka, and N. Nagaosa, A phenomenological theory of superconductor diodes, New J. Phys. **24**, 053014 (2022).

[44] Y.-M. Wu, Z. Wu, and H. Yao, Pair-density-wave and chiral superconductivity in twisted bilayer transition metal dichalcogenides, Phys. Rev. Lett. **130**, 126001 (2023).

[45] M. Salmhofer, C. Honerkamp, W. Metzner, and O. Lauscher, Renormalization group flows into phases with broken symmetry, Prog. Theor. Phys. **112**, 943 (2004).

[46] J. Lichtenstein, D. Sánchez de la Peña, D. Rohe, E. Di Napoli, C. Honerkamp, and S. Maier, High-performance functional renormalization group calculations for interacting fermions, Comput. Phys. Commun. **213**, 100 (2017).

[47] G. A. H. Schober, J. Ehrlich, T. Reckling, and C. Honerkamp, Truncated-unity functional renormalization group for multiband systems with spin-orbit coupling, Front. Phys. **6**, 32 (2018).

[48] W.-S. Wang, Y.-Y. Xiang, Q.-H. Wang, F. Wang, F. Yang, and D.-H. Lee, Functional renormalization group and variational Monte Carlo studies of the electronic instabilities in graphene near $\frac{1}{4}$ doping, Phys. Rev. B **85**, 035414 (2012).

[49] C. Husemann and M. Salmhofer, Efficient parametrization of the vertex function, Ω scheme, and the t, t' Hubbard model at van Hove filling, Phys. Rev. B **79**, 195125 (2009).

[50] J. Reiss, D. Rohe, and W. Metzner, Renormalized mean-field analysis of antiferromagnetism and d-wave superconductivity in the two-dimensional Hubbard model, Phys. Rev. B **75**, 075110 (2007).

[51] W. Metzner and H. Yamase, Phase stiffness in an antiferromagnetic superconductor, Phys. Rev. B **100**, 014504 (2019).